

1 **Modulation of Saharan dust export by the North African dipole**

2
3 Sergio Rodríguez^{1*}, Emilio Cuevas¹, Joseph M. Prospero², Andrés Alastuey³, Xavier Querol³, Javier
4 López-Solano¹, María-Isabel García^{1,4} and Silvia Alonso-Pérez^{1,3,5}

5
6 ¹Izaña Atmospheric Research Centre, AEMET, Santa Cruz de Tenerife, Spain.

7 ²Rosenstiel School of Marine and Atmospheric Science, University of Miami, Miami, Florida, United
8 States.

9 ³Institute of Environmental Assessment and Water Research, CSIC, Barcelona, Spain.

10 ⁴Department of Analytical Chemistry, Nutrition and Food Science, University of La Laguna, Tenerife,
11 Spain

12 ⁵European University of the Canaries, Laureate International Universities. 38300, La Orotava, Tenerife,
13 Spain.

14 *Correspondence to: srodriguezg@aemet.es

15 16 **Abstract**

17 We have studied the relationship between the long term interannual variability in large scale
18 meteorology in western North Africa - the largest and most active dust source worldwide – and Saharan
19 dust export in summer, when enhanced dust mobilization in the hyper-arid Sahara results in maximum
20 dust impacts throughout the North Atlantic. We address this issue by analysing 28-years (1987-2014) of
21 summer averaged dust concentrations at the high altitude Izaña observatory (~2400 m.a.s.l.) in Tenerife
22 Island, satellite and meteorological reanalysis data. Summer meteorological scenario in North Africa
23 (aloft 850 hPa) is characterised by a high over the subtropical Sahara and a low over tropic linked to the
24 monsoon. We measured the variability of this high-low dipole like pattern in terms of the North African
25 Dipole Intensity (NAFDI): the difference of geopotential heights anomalies averaged over the subtropic
26 (30-32°N, Morocco) and the tropic (10-13°N, Bamako region) close to the Atlantic coast (at 5-8°W). We
27 focused on the 700 hPa standard level due to dust export off the coast of North Africa tends to occur
28 between 1 and 5 km.a.s.l. Variability in the NAFDI is associated with displacements of the North African
29 anticyclone over the Sahara and this has implications on winds and dust export. The correlations we
30 found between the 1987 - 2014 summer mean of NAFDI with dust at Izaña, satellite dust observations
31 and meteorological re-analysis data, indicates that increases in the NAFDI (i) results in higher wind
32 speeds at the north of the Inter-Tropical Convergence Zone which are associated with enhanced dust
33 export over the subtropical North Atlantic, (ii) influences the long term variability of the size distribution

34 of exported dust particles (increasing the load of coarse dust) and (iii) are associated with enhanced rains
35 in the tropic and northern shifts of the tropical rain band that may affect southern Sahel. Interannual
36 variability in NAFDI is also connected to spatial distribution of dust over the North Atlantic; high NAFDI
37 summers are associated with major dust export (linked to winds) in the subtropic and minor dust loads in
38 the tropic (linked to higher rainfall), and vice versa. The evolution of the summer NAFDI values since
39 1950 to present days shows connections to climatic variability (through the Sahelian drought, ENSO and
40 winds) that have implications on dust export paths. Efforts to anticipate how dust export may evolve in
41 future decades will require a better understanding on how the large scale meteorological systems
42 represented by the NAFD will evolve.

43

44

45 **1. Introduction**

46 Desert dust aerosols influence global climate by scattering and absorbing radiation (Forster et al.,
47 2007), influencing rainfall (Creamean et al., 2013), and also by modulating ocean-atmosphere CO₂
48 exchange through the deposition of dust which supplies iron, a micronutrient for marine biota (Jickells et
49 al., 2005). Ice core records show increased dust activity during glacial periods when CO₂ was low
50 (Martínez-García et al., 2009). Dense dust hazes often occur between tropical and mid-latitudes over the
51 North Atlantic (Tanaka and Chiba, 2006), with implications also on air quality (Rodríguez et al., 2001;
52 Pérez et al., 2008; Mallone et al., 2011; Díaz et al., 2012). Consequently, there is considerable interest in
53 climate variability, the global distribution of dust (Adams et al., 2012; Ginoux et al., 2012) and dust
54 microphysical properties including particle size which modulates dust impacts (Mahowald et al., 2014),
55 e.g. the interaction with radiation (Otto et al., 2007), iron solubility and supply to the ocean (Baker et al.,
56 2006), its role as cloud and ice nuclei (Welti et al., 2009), and health effects due to dust exposure (Pérez et
57 al., 2008; Mallone et al., 2011; Díaz et al., 2012; Pérez et al., 2014). During atmospheric transport, dust is
58 removed by precipitation and by dry deposition, the latter a process that is strongly size dependent. Dust
59 size variability is observed over time scales of individual dust events (~ days) (Ryder et al., 2013) and in
60 ice cores, over thousands of years, linked to changes in wind speeds, transport pathways and dust sources
61 attributed to climate variability (Delmonte et al., 2004).

62 North Africa is the largest and most active dust source in the world (Ginoux et al., 2004; Huneus
63 et al., 2011; Ginoux et al., 2012). Dust mobilization experiences a marked seasonality. In winter, sources
64 located in southern Sahara and the Sahel (<20°N) are especially active linked to north-easterly dry
65 (Harmattan – trade) winds which prompt dust export across the North African tropical coast (<15°N)
66 (Engelstaedter and Washington, 2007; Haywood et al., 2008; Menut et al., 2009; Marticorena et al.,
67 2010). In summer, the north-east trade winds and the Inter-Tropical Convergence Zone (ITCZ) shift
68 northward, enhancing emissions from Saharan sources and increasing dust export at subtropical latitudes
69 (20-30°N), concurrently the northward shift in the monsoon rain band to southern Sahel tends to decrease
70 Sahelian dust emissions (Engelstaedter and Washington, 2007; Knippertz and Todd, 2010; Ashpole and
71 Washington, 2013, and references therein).

72 There is a major scientific interest in understanding the links between long term variability in
73 North African dust export and climate. Dust sources in part of the Sahel have a hydrological nature
74 (Ginoux et al., 2012); their emissions are affected by the summer variability in rainfalls and also by the
75 North Atlantic Oscillation in winter, and this has had consequences on dust impacts on the tropical North
76 Atlantic detected during, at least, four decades (Prospero and Lamb, 2003; Chiapello et al., 2005). In
77 addition, the increase in commercial agriculture over the last two centuries coupled with droughts has had
78 an impact on Sahelian dust emissions (Mulitza et al., 2010). In contrast the Sahara is a hyper-arid

79 environment (< 200 mm/yr) where natural non hydrological dust sources (i.e. not associated with annual
80 hydrological cycles) prevail (Ginoux et al., 2012), and dust emission variability is mainly controlled by
81 winds (Engelstaedter and Washington, 2007; Ridley et al., 2014). Conceptual model explaining
82 interannual variability in Saharan dust export have been proposed for the winter (e.g. North Atlantic
83 Oscillation by Ginoux et al., 2004; Chiapello et al., 2005), but not for summertime when the highest dust
84 emissions occur in North Africa due to the enhanced activation of the subtropical Saharan sources
85 (Prospero et al., 2003; Ginoux et al., 2004; Chiapello et al., 2005; Tanaka and Chiba, 2006; Engelstaedter
86 and Washington, 2007; Mulitza et al., 2010; Knippertz et al., 2012; Ridley et al., 2014). Doherty et al.
87 (2008) found that the trans-Atlantic dust transport of North African dust to the Caribbean is influenced by
88 displacements in the Azores and Hawaiian anticyclones. In this study we have focused on the links
89 between North African meteorology and dust export.

90 Starting in 1987 we have measured aerosols at the Izaña -Global Atmospheric Watch (GAW) -
91 World Meteorological Organization (WMO) - high-mountain observatory ($28^{\circ}18'N$, $16^{\circ}29'E$, 2367 m.
92 a.s.l.) on Tenerife Island, which frequently lies under the main path of the high altitude Saharan dust
93 outbreaks. At night, when mountain upslope winds cease, Izaña is within the free troposphere airflows,
94 frequently within the dust-laden Saharan Air Layer (SAL) which in summer is typically located at
95 altitudes between ≈ 1 to 5 km a.s.l. (Adams et al., 2012, Nicholson et al., 2013; Tsamalis et al., 2013).
96 Here we report on long term measurements of summertime concentrations of total dust ($dust_T$) (1987-
97 2014) and of dust particles $< 2.5 \mu m$ ($dust_{2.5}$) (2002-2014). Our 28 years observation evidence that there is
98 a significant interannual variability in Saharan dust export in summer. Our research focuses on one key
99 question: *What is the relationship between long term inter-annual variability in Saharan dust export in*
100 *summer and large scale meteorology in North Africa?* For addressing this issue we also used (i) the UV
101 Aerosol Index determined by the Total Ozone Mapping Spectrometer and Ozone Monitor Instrument
102 satellite-borne spectrometers (Herman et al., 1997) for studying long-term and inter-annual spatial
103 distribution of dust and (ii) gridded meteorological National Center for Environmental Prediction /
104 National Center for Atmospheric Research (NCEP/NCAR) re-analysis data (Kalnay et al., 1996) for
105 studying the variability of large scale meteorological processes.

106 In this article, we first perform a brief description of the typical meteorological scenario in
107 western North Africa in the summertime. Then, the concept of the North African dipole is introduced as
108 an approach to characterize how variability in large scale meteorology may influence Saharan dust export.
109 We then assessed how the long term variability in the intensity of the North African dipole has influenced
110 long term Saharan dust export to the free troposphere during 28-years and particle size distribution during
111 13-years. Finally, we assess whether the North African dipole intensity can be used to connect Saharan
112 dust export with climate variability. Here we present connections between dust export and large scale

113 meteorology; further studies will be necessary for understanding the involved meteorological and dust
114 processes.

115
116

117 **2. Methods**

118 **2.1 In-situ dust measurements**

119 We used in-situ dust concentrations data recorded between 1987 and 2014 at Izaña observatory.
120 Here we present a brief description of the methods, details are included in section S1 of the online
121 Supplement.

122 Dust concentrations were obtained by chemical analysis of aerosol samples collected on filter at
123 the flow rate of 30 m³/h. Throughout the almost three decades of observations, several analytical methods
124 have been used for determining soluble species (SO₄⁼, NO₃⁻, NH₄⁺ by ion chromatography and
125 colorimetry), organic and elemental carbon (by TOT), elemental composition (INAA, IPC-AES and IPC-
126 MS) and the content of dust (by the ‘weight of the ash residue after 14-h heating at 500°C’ method and by
127 using the elemental composition data) in the aerosol samples; details of these methods and their use
128 throughout the measurement period are included in Table S1 of the online Supplement. In order to
129 facilitate data comparison with other studies, dust concentrations are reported to mean pressure at sea
130 level (1013 hPa) and normalized in such a way that aluminum accounts for 8% dust (mean content of Al
131 in soils). Here we report on dust concentrations in two size fractions: concentrations of total dust (dust_T)
132 from 1987 to 2014 and of dust particles with an aerodynamic diameter ≤ 2.5 μm (dust_{2.5}) from 2002 to
133 2014 (Rodríguez et al., 2012).

134 Dust concentrations were also calculated with a secondary complementary method based on
135 number size distributions measurements (0.5 to 20 μm) performed with an Optical Particle Counter and
136 an Aerodynamic Particle Sizer. These data were used for determining the aerosol volume concentrations
137 and convert then to bulk aerosol mass concentrations using standard methods (Rodríguez et al., 2012).
138 The good agreement (high linearity and low mean bias, 3-8%) between these two methods (based on
139 chemical analysis and on size distributions) is due to the very low aerosol volume concentrations in the
140 free troposphere during no dust events (typically < 1 to < 3 μg/m³; Rodríguez et al., 2009) and to the fact
141 that the aerosol volume concentrations during dust events are by far dominated by dust, as evidenced by
142 the chemical analysis (Rodríguez et al., 2011) and the ochre color of the aerosol samples (Fig. 1b).

143 These two dust databases (based on chemical and on size distribution methods) were used to
144 assess the consistency of the observed year-to-year variability of dust. During the whole measurement
145 period (25 July 1987 –31 December 2014, excluding the non-measurement period 11 October 1999 - 13
146 February 2002), dust concentrations records are available for 8001 days, which lead to a data availability
147 of 87.3%. This record of aerosol dust concentration is among the longest in the world (after Barbados –

148 started in 1965, Miami – 1972 and American Samoa - 1983) and probably the longest in several aerosol
149 size fractions downwind of a dust large source (Rodríguez et al., 2012).

150

151

152 **2.2 Satellite dust observations**

153 We used UV Aerosol Index (AI) data from the Total Ozone Mapping Spectrometer –TOMS-
154 (1979-2001) and from the Ozone Monitor Instrument –OMI- (2005-2014) spectrometers onboard the
155 satellites Nimbus 7 (TOMS 1979-1993), Earth Probe (TOMS 1996-2001) and Aura (OMI 2005-2014) for
156 studying the spatial and temporal variability of dust. Because of the UV absorption by some minerals (e.g.
157 hematite, goethite), AI has been widely used in dust studies. This is a semi-quantitative parameter; AI
158 values > 1 are considered representative of an important dust load and the frequency of daily AI values $>$
159 1 has been used for dust climatology (Prospero et al., 2002). In North Africa, the AI signal at the north of
160 the summer tropical rain band is due to dust, whereas biomass burning aerosols transported from South
161 Africa contribute to AI signal at the south of the tropical rain band (Prospero et al., 2002). We only
162 analyzed and interpreted the variability in the frequency of daily AI > 1 at the north of the summer
163 tropical rain band. The following data were used:

- 164 • Level 3 TOMS data of the period 1979-2001. TOMS data for the period 2002-2005 were not used due
165 to calibration problems (http://disc.sci.gsfc.nasa.gov/guides/legacy-guides/toms_l3_dataset.gd.shtml).
- 166 • Level 3 OMI data of the period 2005-2014. Although this instrument has experienced the so called
167 “row anomalies” since 2007 (<http://www.knmi.nl/omi/research/product/rowanomaly-background.php>
168), the affected data is not included in the level 3 datasets ([http://disc.sci.gsfc.nasa.gov/Aura/data-
169 holdings/OMI/index.shtml#info](http://disc.sci.gsfc.nasa.gov/Aura/data-holdings/OMI/index.shtml#info))

170 Level 3 daily AI data of TOMS and OMI of summer (August) were downloaded from the
171 Giovanni online data system of the NASA Goddard Earth Sciences Data and Information Services Centre
172 (GES DISC) (<http://disc.sci.gsfc.nasa.gov/>). The consistency of the TOMS and OMI AI data set has
173 already been shown (Li et al., 2009). Consistency between TOMS, OMI and our in situ dust
174 measurements is analyzed in section S3 of the online Supplement (including Fig.S4 and S5).

175

176

177 **2.3 Meteorological reanalysis data**

178 We used gridded meteorological National Center for Environmental Prediction / National Center
179 for Atmospheric Research (NCEP/NCAR) re-analysis data (Kalnay, et al., 1996) for studying the
180 relationship between dust variability and large scale meteorological processes in summer (August). This
181 analysis included geopotential heights, winds and rains used in equation 1 (shown below) and Fig.2, 4 and
182 9.

183 184 185 **2.4 Summer dust season**

186 At Izaña, the summer dust season (impacts of the SAL) typically starts in the second half of July
187 and ends at the beginning of September (section S2 of the online Supplement). The maximum frequency
188 of dust events occurs in August (52% of the August-days as average; Fig. 1). This month is of high
189 interest given that (i) the ITCZ is shifted to the North and consequently (ii) the SAL is exported at the
190 northern most latitude (as evidence the highest frequency of dust impacts at Izaña; Tsamalis et al., 2013)
191 and the maximum rainfall occurs in tropical North Africa (Nicholson et al., 2009). For this reason, we
192 used the August dust averages for studying summer long term dust evolution in the boreal subtropic (Fig.
193 1a). The study of the central month (August) of the summer dust season (excluding July and September)
194 allows characterizing long term evolution in terms of intensity of dust export, avoiding the variability that
195 could be linked to (i) shifts in the beginning (July) or end (September) dates of the dust season or (ii)
196 variability in the location of the ITCZ from July to September. Our data analysis shows that the July to
197 September dust average is dominated by the dust events occurring in August (Fig S3 of the online
198 Supplement). In August 1987-2014, daily dust data were available during 761 days, i.e. a data availability
199 of 94% (excluding the no-measurements period 11 October 1999 - 13 February 2002). In this study we
200 analyze 1987-2014 time series of in-situ dust concentration at Izaña (determined by chemical methods)
201 averaged in all (dust and no-dust) days of August (shown in Fig. 3a and analyzed below). We refer to
202 August as summer. Results are presented in section 4; additional analysis is presented in section S3 of the
203 online Supplement.

204

205

3. North African summer meteorological scenario

Meteorological scenario throughout western North Africa is influenced by the high pressures typical of the subtropical deserts and the so-called western African monsoon (Lafore et al., 2010). Additionally, the formation of the summer Saharan heat low (Lavaysse et al., 2009) in central western Sahara has also implications on meteorological processes, not only related to the development of the wet western African monsoon season in tropical North Africa (Lafore et al., 2009), but also on mobilization, upward transport and export of dust to the North Atlantic at subtropical latitudes (Jones et al., 2003; Flamant et al., 2007; Knippertz and Todd, 2010).

In summer, the vertical structure of the atmosphere over the Sahara is characterized by the Saharan heat low at low levels (surface to 925Pa standard level at $\sim 20^{\circ}\text{N}$) with a confluence of surface ‘northern dry desert Harmattan’ and ‘southern humid monsoon’ winds at its southern margin (Nicholson et al., 2013) in the so-called ITCZ, which in central western Sahara occurs between $18\text{-}20^{\circ}\text{N}$ (Lafore et al., 2010; Pospichal et al., 2010; ITCZ also known as Inter-Tropical-Discontinuity ITD). Monsoon rainfalls occur at southern latitudes ($<15^{\circ}\text{N}$), in a region we will refer as rain band (Nicholson et al., 2009). The Saharan heat low, as a shallow hot depression, enhances subsidence processes due to compensatory downward movement in upper levels (Spengler and Smith, 2008; Canut et al., 2010). The African Easterly Jet (AEJ) forms at altitude between 2 and 6 km between 15 and 20°N due to the thermal wind in the baroclinic zone between the ‘northern hot desert air’ and the ‘cool monsoonal southern airflow’ (Nicholson, 2009, 2013).

Emissions, upward transport and export of dust to the North Atlantic occur in this summer scenario. Dust emission processes occur in a range of scales (Knippertz and Martin, 2012) from (i) synoptic scale (e.g. Harmattan - trade winds, African easterly waves; Jones et al., 2003; Knippertz and Todd, 2010), through (ii) strong winds, convergence and high turbulence associated to the ITCZ (Flamant et al., 2007; Ashpole and Washington, 2013), low-level jets (Knippertz, 2008; Fiedler et al., 2013) and cold pools of mesoscale dry convective systems (particularly over the Sahel; Engelstaedter and Washington, 2007; Lavaysse et al., 2010a, and references therein) including ‘haboob’ storms (Marsham et al., 2008), to (iii) microscale dust devils and dusty plumes (Allen and Washington, 2013). As a consequence of convergence processes close to the ITCZ (Ashpole and Washington, 2013) and because of the convective boundary layer, huge amounts of dust are lifted up to ~ 5 km altitude (Cuesta et al., 2009; Guirado et al., 2014). The easterly subtropical circulation at the south of the North African anticyclone typically present at the altitude of the 700 hPa level and aloft (Font-Tullot, 1950; UK Meteorological Office, 1962), coupled with the divergence linked to the Saharan heat low, and the AEJ (Lavaysse et al., 2010a) expands this dry dusty air mass over the North Atlantic free troposphere resulting

239 in the previously described SAL (Prospero and Carlson, 1972; Tsalamis et al., 2013). Off the coast of
240 North Africa, the summer SAL is found at altitudes between 1 and 5 km (Karyampudi et al., 1999;
241 Immler and Schrems, 2003; Tsamalis et al., 2013; Andrey et al., 2014) due to the westward dust export
242 occurs above the so-called ‘Atlantic inflow’, a layer of cool and stable sea-breeze like inflow present
243 along the subtropical North African coast (Lafore et al., 2010).

244 This brief description illustrates how the presence of the dusty SAL over the North Atlantic is the
245 net result of a set of complex and coupled processes which occur in a wide range of scales and which may
246 also involve (i) feedback mechanisms (e.g. radiative, cloud and rain processes triggered by dust; Lau et
247 al., 2009), (ii) interconnections between processes (e.g. influence of the AEJ-convection-monsoon
248 connections on dust described by Hosseinpour and Wilcox, 2014), (iii) variability in dust emissions due to
249 meteorologically driven variability in soil features (Prospero and Lamb, 2003) and (iv) dust microphysical
250 processes (e.g. size dependent deposition and cloud and radiation interactions; Mahowald et al., 2014).

251

252

253 **4. Results and discussion**

254 **4.1 The North African dipole**

255 We aim to find a simple conceptual model for linking long term variability in Saharan dust export
256 with variability in the large scale meteorology in western North Africa. Because it resemble a dipole, we
257 will refer to the summer meteorological scenario of North Africa - characterized by high pressure in
258 subtropical Sahara (27 - 32 °N over Algeria; Font-Tullot, 1950; UK Meteorological Office, 1962) and low
259 pressure in tropical North Africa (< 15 °N) - the North African Dipole (NAFD). The NAFD is illustrated
260 in the height of the 850 hPa summer average geopotential in Fig. 2. The intensity of this dipole can be
261 measured as the difference of the anomalies of the geopotential height over the subtropic and that over the
262 tropic in North Africa. Because summer dust export to the Atlantic occurs between 1 and 5 km altitude
263 (Prospero and Carlson, 1972; Immler and Schrems, 2003; Tsalamis et al., 2013), with a frequent
264 maximum dust load between 2 and 3 km (Teschen et al., 2009; Cuevas et al., 2014), we paid special
265 attention to the 700 hPa standard level (Nicholson, 2013) at 5 – 8 °W longitude (i.e. close to the Atlantic
266 coast). Thus, in this study we measured the intensity of the NAFD as the difference of the anomalies of
267 the 700hPa geopotential height averaged over central Morocco (30-32°N, 5-7°W) and that over Bamako
268 region in Mali (10-13°N, 6-8°W) by equation 1. Other parameterisations of the NAFD are plausible
269 depending on the study subject. We calculated the NAFD Intensity (NAFDI) with equation 1 using the

270 average values of the 700 hPa geopotential heights in every month of August (31 days average) from
271 1948 to 2014 obtained from the NCEP/NCAR re-analysis (Kalnay, et al., 1996):

272

$$273 \quad NAFDI = \frac{1}{10} ((\phi_{Mo}^y - \langle \phi \rangle_{Mo}) - (\phi_{Ba}^y - \langle \phi \rangle_{Ba})) \quad \text{Equation 1}$$

274 where,

- 275 - ϕ_{Mo}^y is the mean geopotential height at 700hPa averaged in central Morocco region (30-32°N, 5-
276 7°W) in August of year 'y'.
- 277 - $\langle \phi \rangle_{Mo}$ is the mean geopotential height at 700hPa averaged in central Morocco region (30-
278 32°N, 5-7°W) averaged in August months from 1948 to 2012.
- 279 - ϕ_{Ba}^y is the mean geopotential height at 700hPa averaged in Bamako region (10-13°N, 6-8°W) in
280 August of year 'y'.
- 281 - $\langle \phi \rangle_{Ba}$ is the mean geopotential height at 700hPa averaged in Bamako region (10-13°N, 6-
282 8°W) averaged in all August months from 1948 to 2012.
- 283 - $\frac{1}{10}$ is a scale factor.

284

285 The NAFDI (equation 1) is a measure of the inter-annual variability of the dipole intensity and,
286 because of its relationship with the geopotential gradient, it is related with the intensity of the geostrophic
287 North African outflow.

288 Fig 3a shows the time series of the summertime NAFDI values from 1987 to 2014, when it
289 showed values between -3.19 and +2.29. In order to assess how large-scale meteorology changes with
290 NAFDI values, we averaged some meteorological fields during high NAFDI summers and low NAFDI
291 summers (Fig.4a and 4c-4e). The low NAFDI group includes the summers with the four lowest NAFDI
292 values in the period 1987-2014: 1997 (NAFDI = -3.19), 1987 (-2.79), 1996 (-2.04) and 2006 (-1.54). The
293 high NAFDI group includes the summers with the four highest NAFDI values in the period 1987-2014:
294 2012 (+2.29), 2008 (+1.01), 2000 (+0.83) and 1988 (NAFDI= +0.68). Only summers for which satellite
295 AI data are available were considered (i.e. 1993-1995 and 2002-2004 periods were not included in the
296 selection). The spatial distribution of dust was assessed by determining the metric Major Dust Activity
297 Frequency (MDAF): the number of days with AI values > 1 divided by the total number of days with
298 available AI data in % (Fig.4b).

299 The NAFD is illustrated in Fig. 4a with the mean 700hPa geopotential height field during
300 summers of low and of high NAFDI. The core of the northern Saharan anticyclone reinforces over the
301 western Atlas Mountains (~30°N) in high NAFDI summers (Fig.4a2), whereas it weakens and shifts
302 southward to central Algeria (~28°N) in low NAFDI summers (Fig.4a1). Conversely, at the tropical

303 latitude of Bamako (~12N) geopotentials heights are higher during low NAFDI summers (Fig.4a1) than
304 during high NAFDI summers (Fig.4a2).

305

306 **4.2. Long term variability of Saharan dust export**

307 At Izaña we observe a strong interannual variability in dust concentrations (Fig. 3a). In low dust
308 years - 1987, 1997, 2006 and 2007 – mean concentrations were within the range 17 – 30 $\mu\text{g}/\text{m}^3$; in high
309 dust years - 1988, 2008, 2010 and 2012 – the range was 100 - 140 $\mu\text{g}/\text{m}^3$. We associate this variability to
310 the spatial variability of meteorological conditions over North Africa, specifically to the NAFD (Fig.4).
311 The high value of the Pearson correlation coefficient (r) of mean summer dust_T at Izaña with the NAFDI
312 from 1987 to 2014 ($r=0.72$, Fig. 3a) indicates that the dust export is highly sensitive to the dipole intensity
313 (Fig. 5a).

314 The mean wind fields and precipitation rates are shown along with MDAF for low and high
315 NAFDI summers in Fig. 4. There is a significant variability in the spatial distribution of dust over the
316 North Atlantic in high with respect to low NAFDI periods. Increases in the NAFDI are associated with a
317 strengthening of the zonal (easterly) component of continental trade winds north of the ITCZ in a region
318 we define as the subtropical Saharan Stripe (Fig.4c-4d). This strengthening of easterly winds was
319 observed in all standard levels (only shown at 925 and 700 hPa for the sake of brevity) and is associated
320 with a reinforcement of the tropical low to subtropical Saharan high pattern represented by the NAFD
321 (e.g. at the level of 850 hPa, Fig S7 of the online Supplement). The subtropical Saharan Stripe region,
322 which extends from Central Algeria to Western Saharan between 24 and 30 °N, includes important dust
323 sources (Prospero et al., 2002; Schepanski et al., 2009; Rodríguez et al., 2011; Ginoux et al., 2012) which
324 clearly exhibit a greater MDAF during summers with high NAFDI (Fig. 4b2). Long-term (1987-2014)
325 summer mean values of NAFDI and of dust_T at Izaña are highly correlated with the zonal wind in the
326 subtropical Saharan Stripe ($r= 0.6$ to 0.9 , Fig. 6a, where negative correlation indicates reinforcement of
327 westward winds). These correlations reflect the net result of a wide range of dust-related processes
328 (emission, vertical transport, advection to the Atlantic and size dependent deposition during transport).
329 These results are consistent with those of the back-trajectories analysis (Fig. S6 of the online Supplement)

330 The portion of the SAL with a MDAF during more than 40% of the summertime extends from
331 North Africa to 30°W during summers with a low NAFDI (Fig. 4b1); in contrast the region extends to
332 55°W during high NAFDI summers (Fig. 4b2). In high NAFDI summers the SAL also expands northward
333 over the subtropical North Atlantic domain (24 – 35 °N, 9 - 60 °W; Fig. 4b); because of this, the MDAF
334 over the subtropical North Atlantic shows a significant correlation with the NAFDI (1979-2014 $r = 0.73$;
335 Fig. 7a) and with dust records at Izaña (Fig.7b). The positive correlation of NAFDI with the MDAF in the
336 North Atlantic subtropical band (24 – 35 °N, Fig 6b) points to an association between summer-to-summer

337 variability in zonal winds in the subtropical Saharan Stripe (Fig. 4c and 6a) and dust export at subtropical
338 latitudes. Reinforcement of easterly winds during high NAFDI summers is also observed in the AEJ (Fig.
339 4d), which plays a role in the trans-Atlantic dust transport (Jones et al., 2003).

340

341

342 **4.3. Long term variability of dust size distribution**

343 Our dust record in two size fractions was used to assess long term variability in dust size
344 distribution. We found that the NAFDI is correlated with the interannual variability of dust size
345 distribution. Our measurements show pronounced changes in the size distribution of dust particles that are
346 apparently related to wind interannual variability driven by the NAFDI (Fig. 5b). Dust tends to be coarser
347 during high NAFDI years than during low NAFDI years. Observe how the dust_{2.5} to dust_T ratio tends to
348 decrease with the NAFDI increase: ~ 30% in summers with a NAFDI < 0 and down to ~ 20% in summers
349 with a NAFDI > 2 (Fig. 5b). The high amount of coarse (> 2.5 μm) dust during high NAFDI summers
350 may be linked to the activation of dust sources closer to the Atlantic coast and/or faster atmospheric
351 transport due to higher wind speeds. Both processes will reduce the loss rate of larger-size particles due to
352 gravitational deposition during transport (Ryder et al., 2013).

353

354

355 **4.4. Connection of NAFD to climate variability**

356 In this section we assess if the NAFDI could be used for linking long term export of Saharan dust
357 with climate variability during the last decades. Here we present some associations between NAFDI,
358 tropical rains and ENSO that will require future investigations.

359 South of the ITCZ, NAFD is associated with the variability in the tropical monsoon rains. We
360 found that from 1987 to 2014 the interannual variability of the NAFDI is moderately correlated with the
361 precipitation rates over tropical North Africa (Fig. 6c) and with what we defined as Wet Sahel Portion
362 ($r=0.54$, Fig.3d), i.e. the portion of the Sahel region (14-18°N to 17°W-22°E; Fig. 4e) that experienced a
363 precipitation rate ≥ 3 mm/day. High NAFDI summers tend to be associated with enhanced precipitation
364 rates in tropical North Africa and northern shifts in the rain bands that may affect southern Sahel (Fig.4e1,
365 4e2 and 6c). Enhanced dust scavenging in high NAFDI summers may accounts for the negative
366 correlation we observe between the 1987 to 2014 summer mean values of the NAFDI and the MDAF
367 over the Sahel and tropical North Africa (Fig.6b), in a region where rainfall and mixing between the
368 inland monsoon flow and the SAL may have an influence on spatial and temporal distribution of dust
369 (Canut et al., 2010). The low MDAF in the Sahel and in the tropical rain band during high NAFDI
370 summers, with respect to high NAFDI summers, is also clear in Fig. 4b1 and 4b2. This is consistent with

371 the negative correlations between Sahelian rains and dust impacts in the Caribbean found by Prospero and
372 Lamb (2003). The long term (1987-2014) correlation of dust_T at Izaña with the Wet Sahel Portion
373 ($r=0.74$, Fig. 3d) suggests that variability in the Saharan dust export in the subtropic and monsoon tropical
374 rains have been influenced by a common meteorological / climatic mechanism. Observe how high dust_T
375 summers at Izaña have been associated with high Wet Sahel Portion in the last three decades (e.g. 1988,
376 1999, 2010, 2012 and 2013, dust_T= 75 – 140 $\mu\text{g}/\text{m}^3$ and Wet Sahel Portions = 7-15%; Fig 3d) and vice
377 versa (e.g. 1996, 1997, 2006, 2009, 2011, 2014, dust_T= 17 – 45 $\mu\text{g}/\text{m}^3$ and Wet Sahel Portions = 0.8 - 4.5
378 %; Fig 3b). In a shorter time scale (days-to-weeks), this connection of dust export and monsoon rains was
379 also observed by Wilcox et al. (2010), who found that the tropical rain band shifted northward by 1 to 4
380 degrees latitude during westward dust outbreak events accompanied by an acceleration of winds in the
381 northern edge of the EAJ.

382 We also compared the variability of the NAFDI with that of a set of teleconnection indexes and
383 found that the Multivariate ENSO (El Niño Southern Oscillation) Index (MEI), -calculated with sea level
384 pressure, zonal and meridional components of the surface wind, sea surface temperature, surface air
385 temperature and total cloudiness fraction of the sky over the tropical Pacific Ocean - is moderately
386 correlated with the NAFDI ($r=-0.50$) and with dust_T at Izaña (-0.59) (Fig. 1a) (Table S2 of the online
387 Supplement). Because variability in NAFDI is connected to wind at the north of the ITCZ (Fig.6a), these
388 correlations suggest that MEI may be teleconnected to winds over the subtropical Sahara and this would
389 have implications on Saharan dust export. In five of the eight intense ENSO years recorded from 1987 to
390 2014 (green arrows on the top of Fig 3) dust_T concentrations at Izaña were low (1987, 1997, 2006, 2009
391 and 2014, 17-32 $\mu\text{g}/\text{m}^3$; Fig.3a) coupled with rather low zonal winds at 925 mb and 700 mb along the
392 Subtropical Saharan stripe (Fig. 3b and 3c), whereas in the other three intense ENSO years dust_T
393 concentrations were moderate (1991, 1993 and 2002, 47-61 $\mu\text{g}/\text{m}^3$; Fig.3a). In the 1987 - 2014 time
394 series, we can observe that many of the peak dust_T summers are associated with correlated increases in
395 NAFDI and MEI $\cdot(-1)$ (e.g. 1988, 1998 and 2008); however we also observe some peak dust_T summers
396 associated with MEI peaks but rather low NAFDI values (e.g. 2002 and 2010, Fig 3a) and vice versa, i.e.
397 peak dust_T summers associated with NAFDI peaks but rather low MEI values (e.g. 2012). This suggests
398 that NAFDI and MEI may be tracing the dependence of different processes involved in dust export on
399 climate variability (e.g. regional variability in source activation, spatial distribution of dust or altitudinal
400 and latitudinal shifts of the SAL). Observe how long term summer mean dust_T at Izaña exhibits higher
401 linearity with NAFDI + MEI $\cdot(-1)$ (Fig. 5d, $R^2=0.60$) than with either NAFDI (Fig. 5a, $R^2=0.52$) or MEI
402 (Fig. 5c, $R^2=0.34$). The 1987 - 2014 summer mean dust_T at Izaña exhibited a higher correlation with
403 NAFDI + MEI $\cdot(-1)$ ($r=0.77$) than with NAFDI ($r=0.72$) or MEI $\cdot(-1)$ ($r= 0.50$). Teleconnections of dust
404 with several large scale systems were also observed by Doherty et al. (2008), who found that trans-

405 Atlantic transport of dust was teleconnected to displacement of both the Azores and Hawaiian
406 anticyclones. Deficits in the North African tropical rains have also been linked to ENSO (including
407 summer Palmer, 1986; Bhatt, 1989; Janicot et al., 1996; Rowell, 2001), consistent with the correlation
408 found between NAFDI and precipitation rates over tropical North Africa (Fig. 6c) and with the low Wet
409 Sahel Portions we observe in low NAFDI and MEI·(-1) summers (Fig. 3a and 3d). Interannual variability
410 in dust transport in subtropical Asia (Abish and Mohanakumar, 2014) and dust mobilization in sources
411 affected by land use and ephemeral lakes (Ginoux et al., 2012) has also been linked to ENSO.

412 The increase in the concentrations of dust transported to the tropical North Atlantic - at Barbados
413 - since the mid 1970s has been linked to Sahelian droughts (Prospero and Lamb, 2003). Fig. 8a shows the
414 summer NAFDI values from 1950 to 2014. Values of NAFDI were persistently higher prior to the onset
415 of the Sahelian drought – from 1950s to mid 1960s - than since mid 1970s, with the lowest values
416 observed during the most severe part of the drought - from 1980 to 1990 (Fig. 8a). Similarly, summer
417 mean values of zonal wind at 925 mb in the subtropical Saharan Stripe were persistently higher prior to
418 the Sahelian drought (Fig. 8b). This suggests that the meteorological change which occurred in the mid
419 1970s, did not only occur in the Sahel, but also in the subtropical Sahara. Particularly, the high wind
420 speeds in the subtropical Saharan Stripe between mid 1950s and mid 1960s (Fig. 9a) – e.g. compared to
421 the 1980-1990 period (Fig.9b) - may have enhanced dust mobilization in central Sahara (north of the
422 ITCZ, including the subtropical Saharan Stripe). Further studies should address what have been the
423 implications on dust transport paths and impacts over the North Atlantic of such meteorological changes.

424

425 **5. Conclusions**

426 The analysis of the 1987 to 2014 summer mean values of dust concentrations at Izaña observatory
427 (~2400 m.a.s.l. in Tenerife), satellite and meteorological reanalysis data shows that summer Saharan dust
428 export is highly dependent on the variability of the large scale meteorology in North Africa, which is
429 characterised by a high over the subtropical Sahara and a low over tropic linked to the monsoon (at 850
430 hPa and aloft). We referred to this high-low dipole like pattern as North African Dipole (NAFDI) and, in
431 this study, we parameterized its variability in terms of the NAFD Intensity (NAFDI): the difference of
432 geopotential heights anomalies averaged over the subtropic (30-32°N, Morocco) and the tropic (10-13°N,
433 Bamako region) close to the Atlantic coast (at 5-8°W longitude). Because summer dust export off the
434 coast of North Africa tends to occur between 1 and 5 km.a.s.l., we determined the NAFDI at 700 hPa
435 standard level. Other parameterisations of the NAFD are plausible depending on the study subject.

436 We observe significant summer-to-summer variability in the NAFDI, which is associated with
437 shifts in the Saharan high that have implications on winds over the Sahara and on the outflow from North
438 Africa and dust export. Increases in the NAFDI values (i) results in higher wind speeds at the north of the

439 Inter-Tropical Convergence Zone which are associated with enhanced dust export over the subtropical
440 North Atlantic, (ii) influences the size distribution of exported dust particles (increasing the load of coarse
441 dust) and (iii) are associated with enhanced rain in the tropic and northern shifts of the tropical rain band
442 that may affect southern Sahel. Variability in NAFDI is also connected to spatial distribution of dust over
443 the North Atlantic; high NAFDI summers are associated with major winds and dust export in the
444 subtropic and minor dust presence in the tropic (linked to rainfall scavenging), and vice versa.

445 We found connections of NAFDI and dust at Izaña to climate variability. El Niño periods (e.g.
446 1987, 1997, 2006, 2009 and 2014) are generally associated with moderate to low summer mean values of
447 the NAFDI, wind speed at the north of the ITCZ and dust at Izaña, and vice versa during La Niña
448 summers (e.g. 1988, 1998, 1999 and 2010). The 1987 - 2014 summer mean dust records at Izaña showed
449 a higher correlation with NAFDI + MEI·(-1) ($r=0.77$) than with either NAFDI ($r=0.72$) or MEI·(-1) ($r=$
450 0.50). These correlations evidence the need of understanding the processes that links dust with climate
451 variability in the subtropics and tropics.

452 Further studies are necessary to understand how the variability of the summer NAFDI since 1950
453 to present days - associated with high wind speeds over subtropical Saharan dust sources prior to the
454 Sahelian drought and low wind speeds over the subtropical Saharan during the severe part of the drought
455 – may have influenced on the multi-decadal evolution of the dust export paths.

456

457

458 **Acknowledgments**

459 The Izaña GAW program is funded by AEMET and by the Minister of Economy and Competitiveness of
460 Spain (POLLINDUST, CGL2011-26259). We gratefully acknowledge the cooperation of the
461 NOAA/ESRL Physical Sciences Division, the NASA Goddard Earth Science data and Information
462 Services Center and the NOAA Air Resources Laboratory. JMP research is supported by NSF grant AGS-
463 0962256. MIG holds a grant from the Canarian Agency for Research, Innovation and Information Society
464 and the European Social Fund. We thank our colleague Dr. Celia Milford for the comments and
465 suggestions that improved the original manuscript.

466

467

468

470 **References**

- 471 Abish, B., Mohanakumar, K.: Absorbing aerosol variability over the Indian subcontinent and its
472 increasing dependence on ENSO. *Global and Planetary Change* 106, 13–19, 2013.
- 473 Adams, A. M., Prospero, J. M., and Zhang, C.: CALIPSO-derived three-dimensional structure of aerosol
474 over the Atlantic Basin and adjacent continents, *J. Climate*, 25, 6862–6879, doi: 10.1175/JCLI-D-
475 11-00672.1 , 2012.
- 476 Allen, C. J. T., and Washington, R.: The low-level jet dust emission mechanism in the central Sahara:
477 Observations from Bordj-Badji Mokhtar during the June 2011 Fennec Intensive Observation
478 Period, *J. Geophys. Res. Atmos.*, 119, 2990–3015, doi:10.1002/2013JD020594, 2013.
- 479 Andrey, J., Cuevas, E., Parrondo, M.C., Alonso-Pérez, S., Redondas, A., Gil-Ojeda, M.: Quantification of
480 ozone reductions within the Saharan air layer through a 13-year climatologic analysis of ozone
481 profiles, *Atmospheric Environment*, 84, 28-34, 2014.
- 482 Ashpole, I., and Washington, R.: Intraseasonal variability and atmospheric controls on daily dust
483 occurrence frequency over the central and western Sahara during the boreal summer, *J. Geophys.*
484 *Res. Atmos.*, 118, 12,915–12,926, doi:10.1002/2013JD020267, 2013.
- 485 Baker, A. R. and Jickells, T. D.: Mineral particle size as a control on aerosol iron solubility, *Geophys.*
486 *Res. Lett.*, 33, L17608,doi:10.1029/2006GL026557, 2006.
- 487 Ben-Ami, Y., Koren, I., and Altaratz, O.: Patterns of North African dust transport over the Atlantic:
488 winter vs. summer, based on CALIPSO first year data, *Atmos. Chem. Phys.*, 9, 7867-7875,
489 doi:10.5194/acp-9-7867-2009, 2009.
- 490 Bhatt, U., 1989. Circulation regimes of rainfall anomalies in the African–South Asian monsoon belt, *J.*
491 *Clim.*, 2, 1133–1144.
- 492 Canut, G., Lohou, M., Saïd, F., Lohou, F.: Observation of entrainment at the interface between monsoon
493 flow and the Saharan Air Layer. *Q. J. Royal Meteorol. Soc.*, 136, Issue S1, 34–46, 2010
- 494 Chiapello, I., Moulin, C. and Prospero, J. M.: Understanding the long-term variability of African dust
495 transport across the Atlantic as recorded in both Barbados surface concentrations and large-scale
496 Total Ozone Mapping Spectrometer (TOMS) optical thickness, *J. Geophys. Res.*, 110, D18S10,
497 doi:10.1029/2004JD005132, 2005.
- 498 Cowie, S. M., Knippertz, P., Marsham, J. H.: A climatology of dust emission events from northern Africa
499 using long-term surface observations. *Atmos. Chem. Phys. Discuss.*, 14, 7425-7468, 2014.
- 500 Creamean, J. M., Suski, K. J., Rosenfeld, D., Cazorla, A., DeMott, P. J., Sullivan, R. C., White, A. B.,
501 Ralph, F. M., Minnis, P., Comstock, J. M., Tomlinson, J. M. and Prather, K. a: Dust and
502 biological aerosols from the Sahara and Asia influence precipitation in the western U.S., *Science*,
503 339, 1572–1578, doi:10.1126/science.1227279, 2013.
- 504 Cuesta, J., Marsham, J. H., Parker, D. J., and Flamant, C.: Dynamical mechanisms controlling the vertical
505 redistribution of dust and the thermodynamic structure of the West Saharan atmospheric
506 boundary layer during summer, *Atmos. Sci. Lett.*, 10, 34–42, doi:10.1002/asl.207, 2009.

507 Cuevas, E., Camino, C., Benedetti, A., Basart, S., Terradellas, E., Baldasano, J.M., Morcrette, J.J.,
508 Marticorena, B., Goloub, P., Mortier, A., Berjón, A., Hernández, Y., Gil-Ojeda, M., and Schulz,
509 M.: The MACC-II 2007-2008 Reanalysis: Atmospheric Dust Evaluation and Characterization
510 over Northern Africa and Middle East, *Atmos. Chem. Phys.*, 15, 3991-4024, doi:10.5194/acp-15-
511 3991-2015, 2015.

512 Delmonte, B., Petit, J. R., Andersen, K. K., Basile-Doelsch, I., Maggi, V. and Lipenkov, V. Y.: Dust size
513 evidence for opposite regional atmospheric circulation changes over east Antarctica during the
514 last climatic transition, *Clim. Dyn.*, 23, 427–438, doi:10.1007/s00382-004-0450-9, 2004.

515 Díaz, J., Tobías, A. and Linares, C.: Saharan dust and association between particulate matter and case-
516 specific mortality: a case-crossover analysis in Madrid (Spain)., *Environ. Health*, 11, 11,
517 doi:10.1186/1476-069X-11-11, 2012.

518 Draxler, R. R. and Rolph, G. D.: HYSPLIT (HYbrid Single-Particle Lagrangian Integrated Trajectory)
519 Model access via NOAA ARL READY Website (<http://ready.arl.noaa.gov/HYSPLIT.php>)
520 NOAA Air Resources Laboratory, Silver Spring, MD, USA, 2013.

521 Engelstaedter, S. and Washington, R.: Atmospheric controls on the annual cycle of North African dust, *J.*
522 *Geophys. Res.*, 112, D17111, doi:10.1029/2006JD007195, 2007.

523 Fiedler, S., Schepanski, K., Heinold, B., Knippertz, P., and I. Tegen, I.: Climatology of nocturnal low-
524 level jets over North Africa and implications for modeling mineral dust emission, *J. Geophys.*
525 *Res. Atmos.*, 118, 6100–6121, doi:10.1002/jgrd.50394, 2013.

526 Font-Tullos, I.: Las invasiones de aire caliente africano en el Archipiélago Canario, *Revista de Geofísica*,
527 Vol. IX, 36, 334-349, 1950.

528 Forster, P., Ramaswamy, V., Artaxo, P., Berntsen, T., Betts, R., Fahey, D. W., Haywood, J., Lean, J.,
529 Lowe, D. C., Myhre, G., Nganga, J., Prinn, R., Raga, G., Schulz, M. and Dorland, R. Van:
530 *Climate Change 2007: The Physical Science Basis, Contribution of Working Group I to the*
531 *Fourth Assessment Report of the Intergovernmental Panel on Climate Change*, chap. Changes in
532 *Atmospheric Constituents and in Radiative Forcing*, Cambridge University Press, Cambridge, UK
533 and New York, NY, USA, 2007.

534 Ginoux, P., Prospero, J. M., Torres, O. and Chin, M.: Long-term simulation of global dust distribution
535 with the GOCART model: Correlation with North Atlantic Oscillation, *Environ. Modell. Softw.*,
536 19, 113–128, 2004.

537 Ginoux, P., Prospero, J. M., Gill, T. E., Hsu, N. C. and Zhao, M.: Global-scale attribution of
538 anthropogenic and natural dust sources and their emission rates based on MODIS Deep Blue
539 aerosol products, *Rev. Geophys.*, 50, RG3005, doi:10.1029/2012RG000388, 2012.

540 Guirado, C., Cuevas, E., Cachorro, V. E., Toledano, C., Alonso-Pérez, S., Bustos, J. J., Basart, S.,
541 Romero, P. M., Camino, C., Mimouni, M., Zeudmi, L., Goloub, P., Baldasano, J. M., and de
542 Frutos, A. M.: Aerosol characterization at the Saharan AERONET site Tamanrasset, *Atmos.*
543 *Chem. Phys. Discuss.*, 14, 16641-16690, doi:10.5194/acpd-14-16641-2014, 2014.

544 Haywood, J. M., Pelon, J., Formenti, P., et al.: Overview of the dust and Biomass Burning Experiment
545 and African Monsoon Multidisciplinary Analysis Special Observing Period-0, *J. Geophys. Res.*,
546 113, D00C17, doi:10.1029/2008JD010077, 2008.

- 547 Herman, J. R., Bhartia, P. K., Torres, O., Hsu, C., Seftor, C. and Celarier, E.: Global distribution of UV-
548 absorbing aerosols from Nimbus 7 / TOMS data, *J. Geophys. Res.*, 102, 16911-16922,
549 doi:10.1029/96JD03680, 1997.
- 550 Hosseinpour, F., and Wilcox, E.M. Aerosol Interactions with African/ Atlantic Climate Dynamics,
551 *Environmental Research Letter (ERL)*, 9, No. 7, doi:10.1088/1748-9326/9/7/075004, 2014.
- 552 Huneus, N., Schulz, M., Balkanski, Y., Griesfeller, J., Prospero, J., Kinne, S., Bauer, S., Boucher, O.,
553 Chin, M., Dentener, F., Diehl, T., Easter, R., Fillmore, D., Ghan, S., Ginoux, P., Grini, A.,
554 Horowitz, L., Koch, D., Krol, M. C., Landing, W., Liu, X., Mahowald, N., Miller, R., Morcrette,
555 J.-J., Myhre, G., Penner, J., Perlwitz, J., Stier, P., Takemura, T., and Zender, C. S.: Global dust
556 model intercomparison in AeroCom phase I, *Atmos. Chem. Phys.*, 11, 7781-7816,
557 doi:10.5194/acp-11-7781-2011, 2011.
- 558 Immler, F. and Schrems, O.: Vertical profiles, optical and microphysical properties of Saharan dust layers
559 determined by a ship-borne lidar, *Atmos. Chem. Phys.*, 3, 1353-1364, doi:10.5194/acp-3-1353-
560 2003, 2003.
- 561 Janicot, S., V. Moron, and B. Fontaine, Sahel droughts and ENSO dynamics, *Geophys. Res. Lett.*, 23,
562 515–518, 1996.
- 563 Jickells, T. D., An, Z. S., Andersen, K. K., Baker, A. R., Bergametti, G., Brooks, N., Cao, J. J., Boyd, P.
564 W., Duce, R. A., Hunter, K. A., Kawahata, H., Kubilay, N., laRoche, J., Liss, P. S., Mahowald,
565 N., Prospero, J. M., Ridgwell, A. J., Tegen, I. and Torres, R.: Global iron connections between
566 desert dust, ocean biogeochemistry and climate, *Science*, 308, 67–71,
567 doi:10.1126/science.1105959, 2005.
- 568 Jones, C., Mahowald, N., and Luo, C.: The role of easterly waves on African desert dust transport, *J.*
569 *Climate*, 16, 3617–3628, 2003.
- 570 Kalnay, E., Kanamitsu, M., Kistler, R., Collins, W., Deaven, D., Gandin, L., Iredell, M., Saha, S., White,
571 G., Woollen, J., Zhu, Y., Leetmaa, A., Reynolds, R., Chelliah, M., Ebisuzaki, W., Higgins, W.,
572 Janowiak, J., Mo, K. C., Ropelewski, C., Wang, J., Jenne, R., and Joseph, D.: The NCEP/NCAR
573 40-Year Reanalysis Project, *B. Am. Meteorol. Soc.*, 77, 437–471, 1996.
- 574 Karyampudi, V., Palm, S., Reagen, J., Fang, H., Grant, W., Hoff, R., Moulin, C., Pierce, H., Torres, O.,
575 Browell, E., and Melfi, S.: Validation of the saharan dust plume conceptual model using lidar,
576 *Meteosat*, and ECMWF data, *B. Am. Meteorol. Soc.*, 80, 1045–1075, 1999.
- 577 Knippertz, P.: Dust emissions in the West African heat trough—The role of the diurnal cycle and of
578 extratropical disturbances, *Meteorol. Z.*, 17(5), 553–563, 2008.
- 579 Knippertz, P., and Todd, M.C.: The central west Saharan dust hot spot and its relation to African easterly
580 waves and extratropical disturbances, *J. Geophys. Res.*, 115, D12117,
581 doi:10.1029/2009JD012819, 2010.
- 582 Knippertz, P. and Todd, M.C.: Mineral dust aerosols over the Sahara: Meteorological controls on
583 emission and transport and implications for modelling. *Reviews of Geophysics*, 50, RG1007,
584 DOI: 10.1029/2011RG000362, 2012.

- 585 Knippertz, P. and Todd, M. C.: Mineral dust aerosols over the Sahara: Meteorological controls on
586 emission and transport and implications for modeling, *Rev. Geophys.*, 50, RG1007,
587 doi:10.1029/2011RG000362, 2012.
- 588 Lafore, J.-P., Flamant, C. Giraud, V. Guichard, F., Knippertz, P., Mahfouf, J.-F., Mascart, P., Williams,
589 E.R.: Introduction to the AMMA Special Issue on ‘Advances in understanding
590 atmospheric processes over West Africa through the AMMA field campaign’, *Q. J. R.
591 Meteorol. Soc.* 136 (S1), pages 2–7, 2010.
- 592 Lavaysse, C., Flamant, C., Janicot, S., Parker, D. J., Lafore, J.-P., Sultan, B., and Pelon, J: Seasonal
593 evolution of the West African heat low: A climatological perspective, *Clim. Dynam.*, 33(2–3),
594 313–330, doi:10.1007/s00382-009-0553-4, 2009.
- 595 Lavaysse, C., Flamant, C., and Janicot, S.: Regional-scale convection patterns during strong and weak
596 phases of the Saharan heat low, *Atmos. Sci. Lett.*, 11(4), 255–264, doi:10.1002/asl.284, 2010a.
- 597 Lavaysse, C., Flamant, C., Janicot, S., and Knippertz, P.: Links between African easterly waves,
598 midlatitude circulation and intraseasonal pulsations of the West African heat low, *Q. J. R.
599 Meteorol. Soc.*, 136(S1), 141–158, doi:10.1002/qj.555, 2010b.
- 600 Li, J., Carlson, B. E. and Lacis, A. A.: A study on the temporal and spatial variability of absorbing
601 aerosols using Total Ozone Mapping Spectrometer and Ozone Monitoring Instrument Aerosol
602 Index data, *J. Geophys. Res.*, 114, D09213, doi:10.1029/2008JD011278, 2009.
- 603 Lucio, P.S., Baldicero Molion, L.C., Avila Valadão, C. E., Conde, F.C., Ramos, A.M., Dias de Melo,
604 M.L.: Dynamical Outlines of the Rainfall Variability and the ITCZ Role over the West Sahel,
605 *Atmospheric and Climate Sciences*, 2, 337-350, doi:10.4236/acs.2012.23030, 2012.
- 606 Mahowald, N., Albani, S., Kok, J. F., Engelstaeder, S., Scanza, R., Ward, D. S. and Flanner, M. G.: The
607 size distribution of desert dust aerosols and its impact on the Earth system, *Aeolian Res.*,
608 doi:10.1016/j.aeolia.2013.09.002, 2014, in press.
- 609 Mallone, S., Stafoggia, M., Faustini, A., Gobbi, J. P., Marconi, A., and Forastiere, F.: Saharan dust and
610 associations between particulate matter and daily mortality in Rome, Italy, *Environ. Health
611 Perspect.*, 119, 1409–1414, doi:10.1289/ehp.1003026, 2011.
- 612 Marsham, J., Parker, D. Grams, C., Taylor, C., and Haywood, J.: Uplift of Saharan dust south of the
613 intertropical discontinuity, *J. Geophys. Res.*, 113, D21102, doi:10.1029/2008JD009844, 2008.
- 614 Marticorena, B., Chatenet, B., Rajot, J. L., Traoré, S., Coulibaly, M., Diallo, A., Koné, I., Maman, A.,
615 NDiaye, T., and Zakou, A.: Temporal variability of mineral dust concentrations over West Africa:
616 analyses of a pluriannual monitoring from the AMMA Sahelian Dust Transect, *Atmos. Chem.
617 Phys.*, 10, 8899-8915, doi:10.5194/acp-10-8899-2010, 2010.
- 618 Martínez-García, A., Rosell-Melé, A., Geibert, W., Gersonde, R., Masqué, P., Gaspari, V. and Barbante,
619 C.: Links between iron supply, marine productivity, sea surface temperature, and CO₂ over the
620 last 1.1 Ma, *Paleoceanography*, 24, PA1207, doi:10.1029/2008PA001657, 2009.

- 621 Menut, L., Chiapello, I., and Moulin, C.: Predictability of mineral dust concentrations: The African
622 Monsoon Multidisciplinary Analysis first short observation period forecasted with CHIMERE-
623 DUST, *J. Geophys. Res.*, 114, D07202, doi:10.1029/2008JD010523, 2009.
- 624 Mulitza, S., Heslop, D., Pittauerova, D., Fischer, H. W., Meyer, I., Stuut, J.-B., Zabel, M., Mollenhauer,
625 G., Collins, J. A., Kuhnert, H., and Schulz, M.: Increase in African dust flux at the onset of
626 commercial agriculture in the Sahel region, *Nature*, 466, 226– 228, doi: 10.1038/nature09213 ,
627 2010.
- 628 Nicholson, S. E.: A revised picture of the structure of the “monsoon” and land ITCZ over West Africa,
629 *Clim. Dyn.*, 32, 1155–1171, doi:10.1007/s00382-008-0514-3, 2009.
- 630 Nicholson, S. E.: The West African Sahel: A Review of Recent Studies on the Rainfall Regime and Its
631 Interannual Variability. *ISRN-Meteorology*, 2013, 453521, 32,
632 <http://dx.doi.org/10.1155/2013/453521>, 2013.
- 633 Otto, S., de Reus, M., Trautmann, T., Thomas, A., Wendisch, M., and Borrmann, S.: Atmospheric
634 radiative effects of an in situ measured Saharan dust plume and the role of large particles, *Atmos.*
635 *Chem. Phys.*, 7, 4887-4903, doi:10.5194/acp-7-4887-2007, 2007.
- 636 Palmer, T., Influence of the Atlantic, Pacific and Indian oceans on Sahel rainfall, *Nature*, 322, 251–253,
637 1986.
- 638 Pérez, L., Tobías, A., Querol, X., Künzli, N., Pey, J., Alastuey, A., Viana, M., Valero, N., González-
639 Cabré, M. and Sunyer, J.: Coarse particles from Saharan dust and daily mortality., *Epidemiology*,
640 19, 800–807, doi:10.1097/EDE.0b013e31818131cf, 2008.
- 641 Pérez García-Pando, C., Stanton, M.C., Diggle, P.J., Trzaska, S., Miller, R.L., Perlwitz, J.P., Baldasano,
642 J.M., Cuevas, E., Ceccato, P., Yaka, P., and Thomson, M.C.: Soil Dust Aerosols and Wind as
643 Predictors of Seasonal Meningitis Incidence in Niger, *Environmental Health Perspectives*
644 doi:10.1289/ehp.1306640, 2014.
- 645 Pospichal, B., Karam, D.B., Crewell, S., Flamant, C., Hünerbein, A., Bock, O., Saïde, F.: Diurnal cycle
646 of the intertropical discontinuity over West Africa analysed by remote sensing and mesoscale
647 modelling. *Q. J. R. Meteorol. Soc.* 136(s1): 92–106, 2010.
- 648 Prospero, J. M., Ginoux, P., Torres, O., Nicholson, S. E., and Gill, T. E.: Environmental characterization
649 of global sources of atmospheric soil dust identified with the Nimbus 7 Total Ozone Mapping
650 Spectrometer (TOMS) absorbing aerosol product, *Rev. Geophys.*, 40,
651 doi:10.1029/2000RG000095 1–31, 2002.
- 652 Prospero, J. M. and Lamb, P. J.: African droughts and dust transport to the Caribbean: climate change
653 implications., *Science*, 302, 1024–1027, doi:10.1126/science.1089915, 2003.
- 654 Prospero, J. M., F.-X. Collard, J. Molinié, and A. Jeannot: Characterizing the annual cycle of African dust
655 transport to the Caribbean Basin and South America and its impact on the environment and air
656 quality, *Global Biogeochem. Cycles*, 29, doi:10.1002/2013GB004802, 2014.

- 657 Ridley, D. A., Heald, C. L., and Prospero, J. M.: What controls the recent changes in African mineral dust
658 aerosol across the Atlantic?, *Atmos. Chem. Phys.*, 14, 5735-5747, doi:10.5194/acp-14-5735-
659 2014, 2014.
- 660 Rodríguez, S., Querol, X., Alastuey, A., Kallos, G., and Kakaliagou, O.: Saharan dust contributions to
661 PM10 and TSP levels in Southern and Eastern Spain, *Atmos. Environ.*, 35, 2433–2447,
662 doi:10.1016/S1352-2310(00)00496-9, 2001.
- 663 Rodríguez, S., González, Y., Cuevas, E., Ramos, R., Romero, P. M., Abreu-Afonso, J., and Redondas, A.:
664 Atmospheric nanoparticle observations in the low free troposphere during upward orographic
665 flows at Izaña Mountain Observatory, *Atmos. Chem. Phys.*, 9, 6319-6335, doi:10.5194/acp-9-
666 6319-2009, 2009.
- 667 Rodríguez, S., Alastuey, A., Alonso-Pérez, S., Querol, X., Cuevas, E., Abreu-Afonso, J., Viana, M.,
668 Pérez, N., Pandolfi, M., and de la Rosa, J.: Transport of desert dust mixed with North African
669 industrial pollutants in the subtropical Saharan Air Layer, *Atmos. Chem. Phys.*, 11, 6663-6685,
670 doi:10.5194/acp-11-6663-2011, 2011.
- 671 Rodríguez, S., Alastuey, A. and Querol, X.: A review of methods for long term in situ characterization of
672 aerosol dust, *Aeolian Res.*, 6, 55–74, doi:10.1016/j.aeolia.2012.07.004, 2012.
- 673 Rowell, D., Teleconnections between the tropical Pacific and the Sahel, *Q. J. R. Meteorol. Soc.*, 127,
674 1683–1706, 2001.
- 675 Ryder, C. L., Highwood, E. J., Lai, T. M., Sodemann, H. and Marsham, J. H.: Impact of atmospheric
676 transport on the evolution of microphysical and optical properties of Saharan dust, *Geophys. Res.*
677 *Lett.*, 40, 2433–2438, doi:10.1002/grl.50482, 2013.
- 678 Schepanski, K., Tegen, I., Todd, M. C., Heinold, B., Bönisch, G., Laurent, B., and Macke, A.:
679 Meteorological processes forcing Saharan dust emission inferred from MSG-SEVIRI
680 observations of subdaily dust source activation and numerical models, *J. Geophys. Res.*, 114,
681 D10201, doi:10.1029/2008JD010325, 2009.
- 682 Spengler, T., Smith, R.K.: 2008. The dynamics of heat lows over flat terrain. *Q. J. R. Meteorol. Soc.* 134:
683 2157–2172.
- 684 Tanaka TY, Chiba M.: A numerical study of the contribution of dust source regions to the global dust
685 budget, *Glob. Planet Change* 2006;52:88-104.
- 686 Tesche, M., Ansmann, A., Müller, D., Althausen, D., Mattis, I., Heese, B., Freudenthaler, V., Wiegner,
687 M., Esselborn, M., Pisani, G., and Knippertz, P.: Vertical profiling of saharan dust with Raman
688 lidars and airborne HSRL in southern Morocco during SAMUM, *Tellus*, B61, 144–164,
689 doi:10.1111/j.1600-0889.2008.00390.x, 2009.
- 690 Tsamalis, C., Chédin, A., Pelon, J., Capelle, V.: The seasonal vertical distribution of the Saharan Air
691 Layer and its modulation by the wind. *Atmos. Chem. Phys.*, 13, 11235–11257, 2013.
- 692 UK Meteorological Office, 1962. *Weather in the Mediterranean*, Vol. I, 2nd Edition. General Meteorology
693 HM Stat. Office, London.

694 Welti, A., Lüönd, F., Stetzer, O. and Lohmann, U.: Influence of particle size on the ice nucleating ability
695 of mineral dusts, *Atmos. Chem. Phys.*, 9, 6705-6715, doi:10.5194/acp-9-6705-2009, 2009.

696 Wilcox, E. M., Lau, K. M., and Kim, K.-M.: A northward shift of the North Atlantic Ocean Intertropical
697 Convergence Zone in response to summertime Saharan dust outbreaks, *Geophys. Res. Lett.*, 37,
698 L04804, doi:10.1029/2009GL041774, 2010.

699

700 **Figure 1.** Saharan dust observations in Izaña. A) Frequency of dust events ($> 10 \mu\text{g}/\text{m}^3$) in Izaña in the
701 period 1987-2014. B) Batch of filters with aerosol samples collected at Izaña for illustrating their
702 typical ochre colour due to dust.

703 **Figure 2.** Mean height of the 850 hPa geopotential over North Africa in summer (August).

704 **Figure 3.** Long term evolution (1987-2014) of summer dust and meteorology. Summer mean values of
705 dust_T concentrations at Izaña (black dot, A-D), MEI (green line, A), NAFDI (red triangle, A), zonal wind
706 at 925 mb in the Subtropical Saharan stripe (25-28 °N, 7°W - 2°E, B), zonal wind at 700 mb averaged in
707 the Subtropical Saharan stripe to Tenerife corridor (25-28 °N, 16°W - 2°E, C) and Wet Sahel Portion (blue
708 dot) from 1987 to 2014. Green and red arrows highlight moderate and intense ENSO and La Niña
709 summers, respectively (<http://www.cpc.ncep.noaa.gov>).

710 **Figure 4.** North African dipole and spatial distribution of dust and meteorological fields averaged in low
711 and high NAFDI summers. Low NAFDI group includes the summers with the four lowest NAFDI values
712 in the period 1987-2014 (1987, 1996, 1997 and 2006 = -2.79, -2.04, -3.19 and -1.54, respectively). High
713 NAFDI group includes the summers with the four highest NAFDI values in the period 1987-2014 (1988,
714 2000, 2008 and 2012 = +0.68, +0.83, +1.01 and +2.29, respectively). Only summers for which satellite AI
715 data are available were considered for this Low and High NAFDI summers selection (i.e. 1993-1995 and
716 2002-2004 were not included). A) height of 700hPa geopotential highlighting the location of the two
717 regions used for determining the NAFDI. B) MDAF at the north of the rain band (data at the south of the
718 tropical rain band is due to biomass burning aerosols from Southern Africa) (Prospero et al., 2002). Mean
719 winds at (C) 925hPa (≈ 800 m.a.s.l.) and (D) 700hPa (≈ 3000 m.a.s.l.). E) mean precipitation rates. The
720 location of the Inter-Tropical Convergence Zone (ITCZ), the Subtropical Saharan Stripe (SSS), the
721 African Easterly Jet (AEJ) and the Subtropical North Atlantic (SNA) are highlighted.

722 **Figure 5.** Scatter plot of dust versus NAFDI and MEI. Summer mean dust_T at Izaña (1987-2014) versus
723 NAFDI (A), MEI (C) and NAFDI + MEI(-1) (D), and summer mean dust_{2,5-to-dust_T} ratio (B, 2002-2014)
724 versus NAFDI. Different symbols are used for the summer mean data of 2002 (black triangle), 2010 (grey
725 triangle) and 2012 (white filled symbol) for exemplifying how some data may have different associations
726 with NAFDI and MEI.

727 **Figure 6.** Influence of the NAFD strengthening on zonal winds, spatial distribution of dust and
728 precipitation rate. Correlation coefficient between long term (1987-2012) summer NAFDI and (A) zonal
729 wind (B) MDAF and (C) precipitation rate. The Inter-Tropical Convergence Zone (ITCZ) and the
730 subtropical Saharan Stripe (SSS) are highlighted. Arrows indicate (A) zonal wind direction and (B)
731 relevant airflows for dust mobilization.

732 **Figure 7.** Scatter plot of summer dust activity in the subtropical North Atlantic versus the NAFDI.
733 MDAF in the Subtropical North Atlantic (SNA) versus the NAFDI (A) and versus dust_T at Izaña (B).

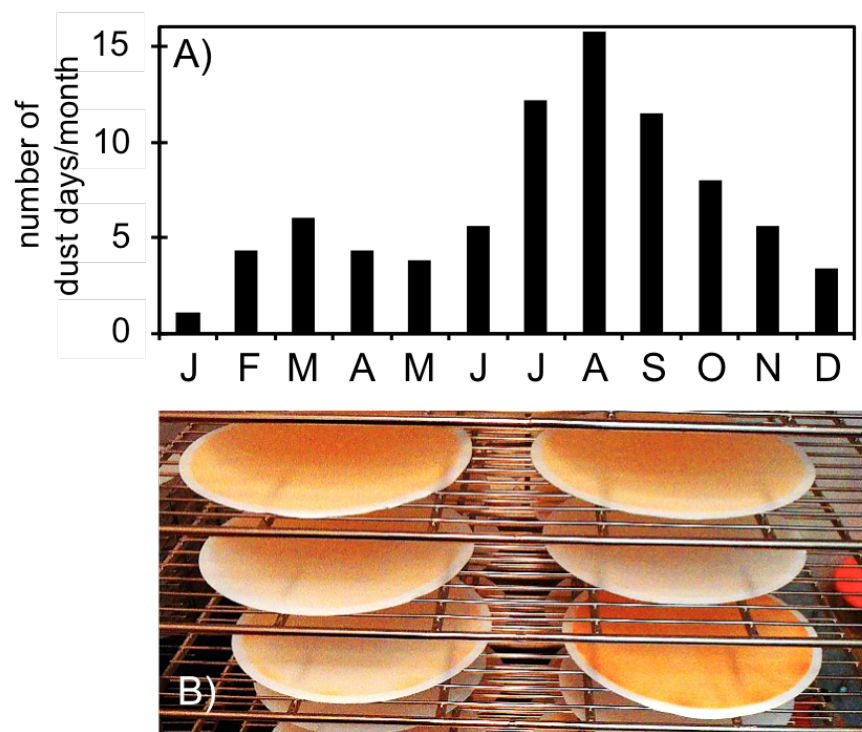
734 Measurements of the TOMS (red circle) and OMI (blue dot) satellite borne sensors were used. The R^2
735 coefficient of the linear fitting is included.

736

737 **Figure 8.** Summer mean values of NAFDI (red triangle, A), $dust_T$ at Izaña (black dot, A) and zonal wind
738 at 925 mb in the Subtropical Saharan stripe (25-28 °N, 7°W - 2°E, B). Period of plentiful rains and severe
739 drought in the Sahel are highlighted according to Lucio et al. (2012).

740 **Figure 9.** Mean winds at 925hPa (\approx 800 m.a.s.l.) in the 1957-1967 (plentiful rains in the Sahel) and the
741 1980-1990 (severe Sahelian drought) decades

742



743

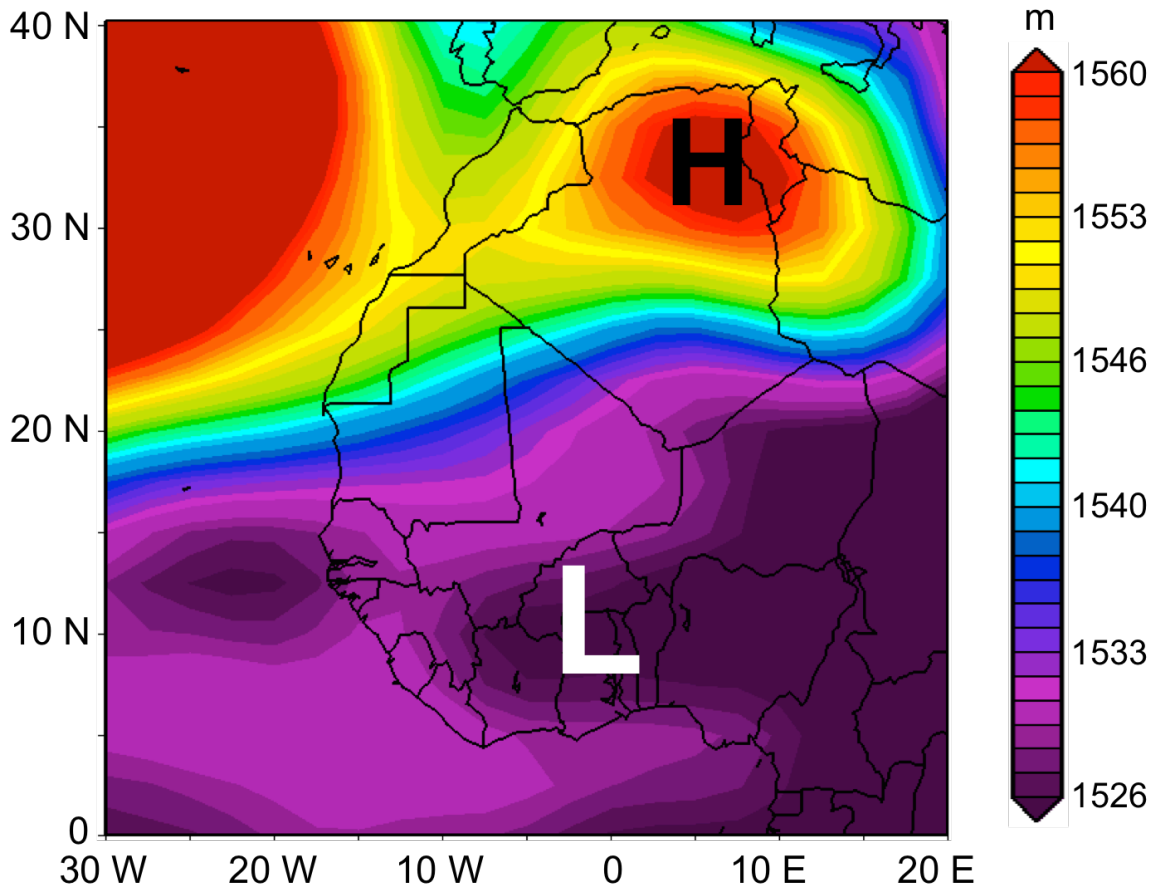
744

745

746

Figure 1.

747



748

749

750

Figure 2.

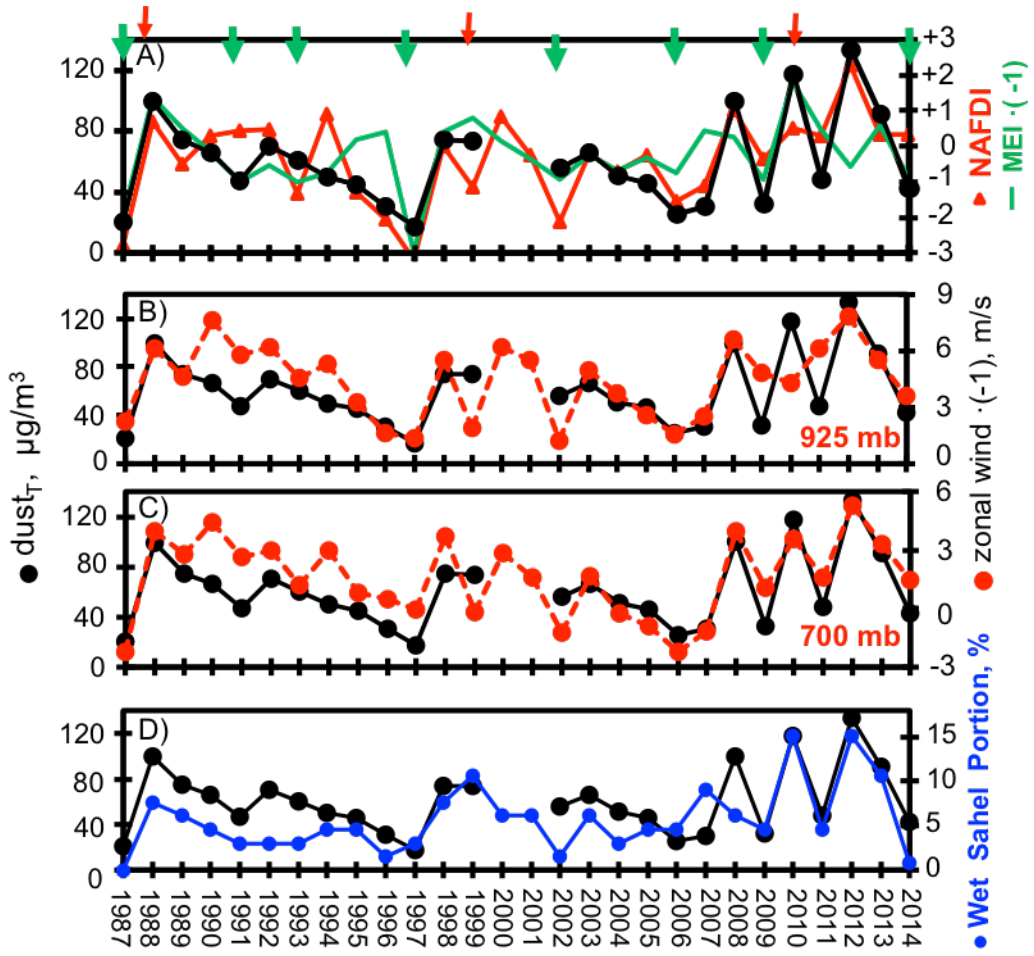


Figure 3

751

752

753

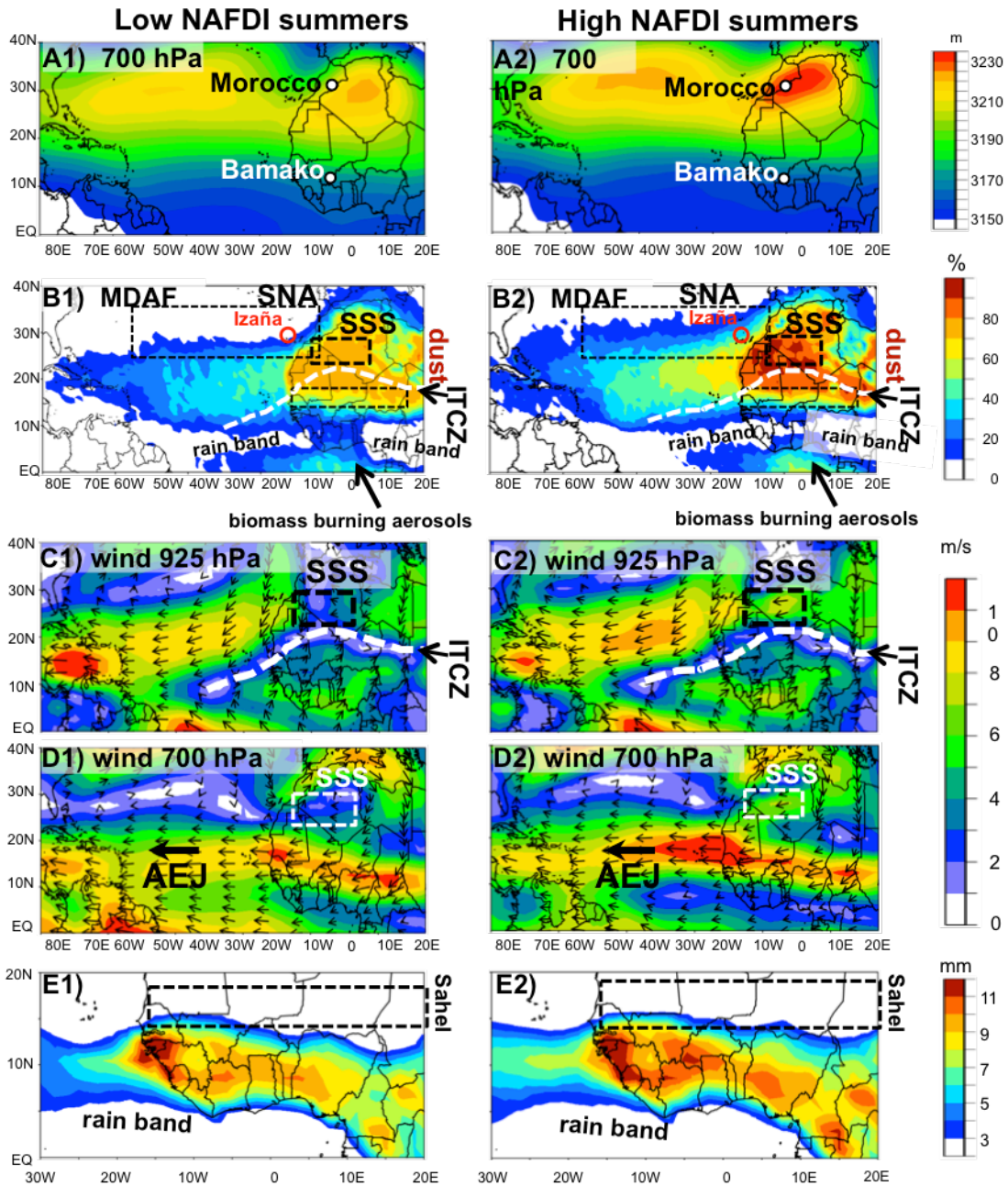


Figure 4.

754
755
756

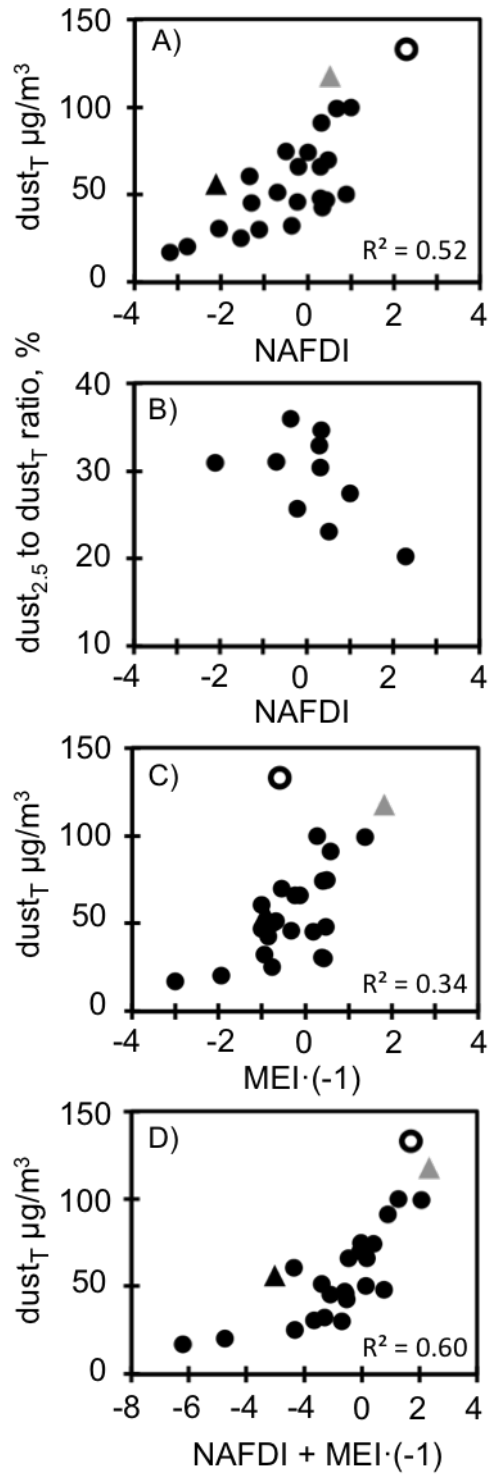


Figure 5.

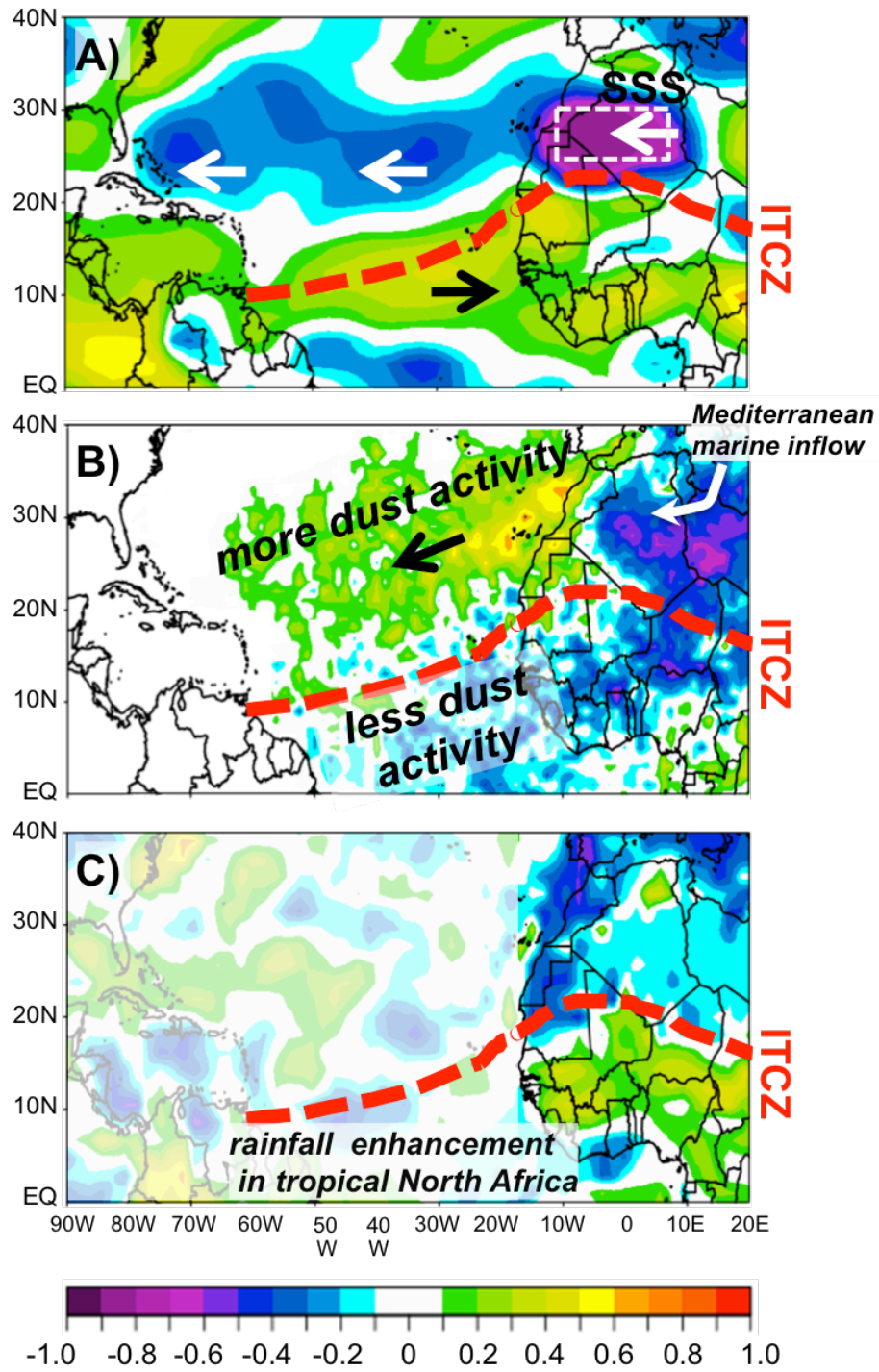
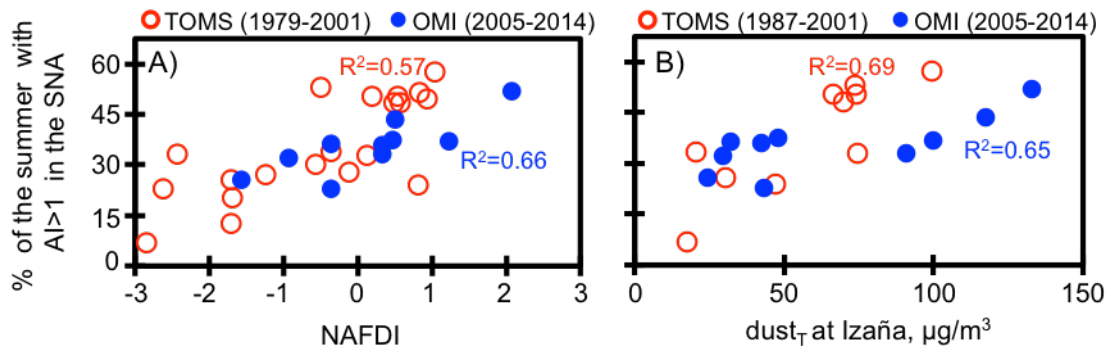


Figure 6.

766



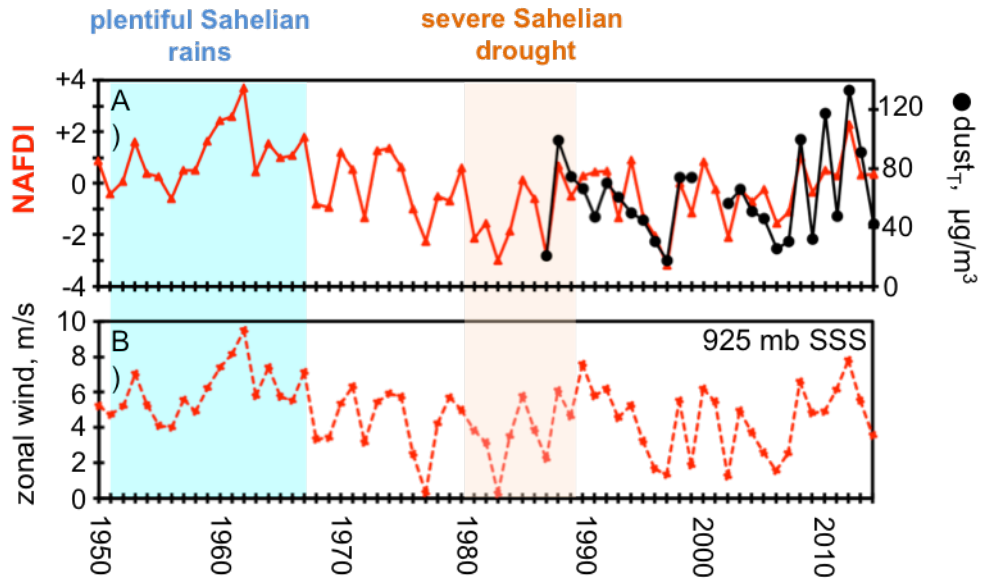
767

768

769

770

Figure 7.



771

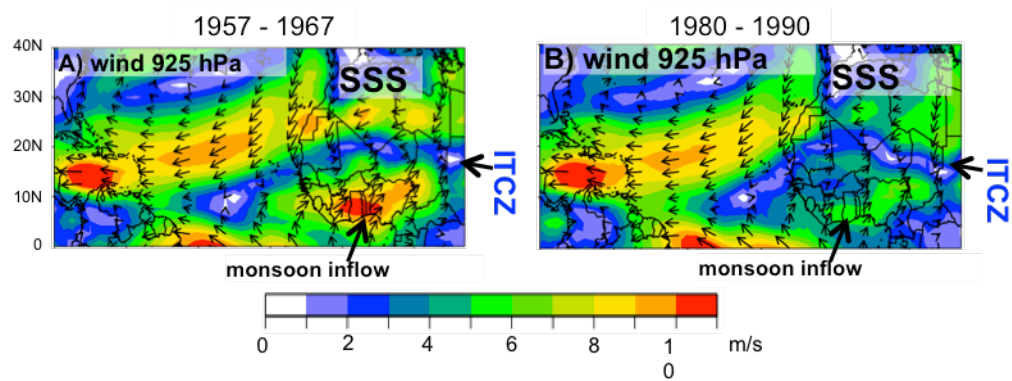
772

773

774

Figure 8.

775



776

777

778

779

780

781

Figure 9.